The non-conservation of potential vorticity by a dynamical core compared with the effects of parametrized physical processes

RMetS
Royal Meteorological Society

The non-conservation of potential vorticity by a dynamical core compared with the effects of parametrized physical processes

L. Saffin,* J. Methven and S. L. Gray
Department of Meteorology, University of Reading, UK

*Correspondence to: L Saffin, Department of Meteorology, University of Reading, Reading RG6 6BB, UK.
E-mail: l.saffin@pgr.reading.ac.uk
The copyright line for this article was changed on 2 March 2016 after original online publication.

Numerical models of the atmosphere combine a dynamical core, which approximates solutions to the adiabatic, frictionless governing equations for fluid dynamics, with tendencies arising from the parametrization of other physical processes. Since potential vorticity (PV) is conserved following fluid flow in adiabatic, frictionless circumstances, it is possible to isolate the effects of non-conservative processes by accumulating PV changes in an air-mass-relative framework. This 'PV tracer technique' is used to accumulate separately the effects on PV of each of the different non-conservative processes represented in a numerical model of the atmosphere. Dynamical cores are not exactly conservative because they introduce, explicitly or implicitly, some level of dissipation and adjustment of prognostic model variables which acts to modify PV. Here, the PV tracers technique is extended to diagnose the cumulative effect of the non-conservation of PV by a dynamical core and its characteristics relative to the PV modification by parametrized physical processes.

Quantification using the Met Office Unified Model reveals that the magnitude of the non-conservation of PV by the dynamical core is comparable to those from physical processes. Moreover, the residual of the PV budget, when tracing the effects of the dynamical core and physical processes, is at least an order of magnitude smaller than the PV tracers associated with the most active physical processes. The implication of this work is that the non-conservation of PV by a dynamical core can be assessed in case-studies with a full suite of physics parametrizations and directly compared with the PV modification by parametrized physical processes. The non-conservation of PV by the dynamical core is shown to move the position of the extratropical tropopause while the parametrized physical processes have a lesser effect at the tropopause level.

Key Words: diabatic processes; numerical weather prediction; tracers; model error

Received 7 October 2015; Revised 7 December 2015; Accepted 16 December 2015; Published online in Wiley Online Library

1. Introduction

Potential vorticity (PV) thinking has become a key concept in dynamical meteorology. PV has two key properties, conservation (Ertel, 1942) and invertibility as discussed in Hoskins *et al.* (1985). Conservation means that, in the absence of diabatic and frictional processes, PV is advected like a tracer. Invertibility means that the PV distribution, with appropriate boundary conditions, is sufficient to diagnose all of the dry dynamical variables to the approximation of a given balance condition. The usefulness of PV thinking depends on the accuracy of the balanced dynamics. Davis *et al.* (1996) demonstrated that most of the dynamics of an intense extratropical cyclone could be quantified using the balance equations of Charney (1955). McIntyre and Norton (2000) showed that higher-order PV-based balanced models were capable of producing simulations 'remarkably similar' to the full unbalanced equations for shallow-water simulations.

Considering the PV conservation in a numerical model of the atmosphere, Davis *et al.* (1993) partitioned PV into a set of tracer diagnostics to explicitly integrate the cumulative effects of parametrized physical processes in a study of cyclogenesis. Combined with the piecewise PV inversion method of Davis and Emanuel (1991), this allowed them to assess the impact of non-conservative processes on a cyclone's circulation. The PV diagnostics did have limitations. Davis *et al.* (1993) noted differences between the PV tracers and the PV diagnosed from model variables and attributed this to numerical truncation

errors in updating PV. Stoelinga (1996) discussed this difference in more detail and attributed it to the difference between the explicit PV integration and the model dynamics which are not designed to conserve PV exactly.

Zhang *et al.* (2008) demonstrated that inconsistencies between tracer advection and the dynamical core of an atmospheric model can produce significant biases in modelling chemical transport. Whitehead *et al.* (2015) assessed the consistency of several dynamical cores with their respective tracer advection schemes by using PV in an idealised baroclinic wave test. In this test there is no diabatic heating or friction, so the only source of PV non-conservation is dissipation, implicit or explicit, induced by the dynamical core. Whitehead *et al.* (2015) tested the consistency of this dissipation with the dissipation induced by the tracer advection scheme for a range of dynamical cores and demonstrated that each dynamical core produces values of PV inconsistent with the tracer advection scheme, but with structure and amplitude differing between dynamical cores. Whitehead *et al.* (2015) used the consistency between a dynamical PV and a tracer of PV to rank the different dynamical cores.

Tracers of PV have been used for two things: assessing the dynamical impacts of parametrized physical processes, and diagnosing inconsistencies between dynamical cores and tracer advection schemes. In this study we demonstrate that, by extending the PV diagnostics of Davis *et al.* (1993), we can explicitly diagnose the inconsistency in PV (defined by Whitehead *et al.*, 2015) in a simulation which also has parametrized physical processes. We show that this 'dynamics-tracer inconsistency' is comparable to the effects on PV of parametrized physical processes for a case-study with the Met Office's Unified Model (MetUM) and that the majority of the 'dynamics-tracer inconsistency' in the MetUM can be attributed to non-conservation of PV by the dynamical core.

We will consider the effects of the non-conservation of PV by the dynamical core in the context of previous studies with the PV tracers in the MetUM. Using the PV tracers, Chagnon *et al.* (2013) identified a dipole in diabatically modified PV across the extratropical tropopause for a case-study of an extratropical cyclone. The extratropical tropopause corresponds to a sharp gradient in PV and can be defined as a surface of PV with 2 PVU (PV units) (Reed, 1955; Hoskins *et al.*, 1985). The tropopause dipole consisted of positive diabatically generated PV in the stratosphere and negative diabatically generated PV in the troposphere either side of the 2 PVU surface, suggesting a sharpening of the tropopause PV gradient due to non-conservative processes (Chagnon *et al.*, 2013). Chagnon and Gray (2015) showed that a tropopause dipole was also present in three other case-studies of extratropical cyclones. We will show that the non-conservation of PV by the dynamical core of the MetUM acts to diminish the tropopause dipole in our case-study.

The structure of the article is as follows. Section 2 describes the methods of analysis as well as introducing the case-study. Section 3 presents the results obtained from a detailed investigation of the PV budget in the MetUM and the implication for the tropopause dipole. Section 4 provides a summary and discussion of the results. A large amount of specific notation is used in this article so a notation table is provided in an Appendix.

2. Methodology

In this section we describe the methods used in this study. A simulation was performed using the MetUM version 7.3. Details of the MetUM are provided below with a description of the PV tracers method and the case-study used. Offline trajectory calculations have also been used in this study and details of the method are provided at the end of this section.

2.1. Met Office Unified Model

The MetUM is an operational numerical weather prediction model (Davies *et al.*, 2005). The dynamical core of the MetUM approximates a two-time-level, semi-implicit, semi-Lagrangian solution to the governing equations of the atmosphere. The prognostic variables in the MetUM are wind ($\mathbf{u} = (u, v, w)$), potential temperature (θ), the mixing ratios of moisture variables (specific humidity, cloud ice and cloud liquid), density (ρ) and Exner pressure (Π). The variables in the MetUM are placed on an Arakawa C-grid with Charney–Phillips staggering in the vertical.

The MetUM contains various parametrizations to account for physical processes that are either not resolved or not represented within the dynamical core: radiation (Edwards and Slingo, 1996); microphysics (Wilson and Ballard, 1999); non-orographic gravity-wave drag (Scaife *et al.*, 2002) and orographic gravity-wave drag (Webster *et al.*, 2003); convection (Gregory and Rowntree, 1990); and turbulent mixing represented by the boundary-layer scheme of Lock *et al.* (2000).

The simulation in this paper uses a previously operational limited-area domain known as the NAE (North Atlantic and Europe) domain nested within a global domain using the method described in Davies (2013); Figure 2 below shows the extent of the NAE domain. The lateral boundary conditions used were produced from the operational runs of the global model and the start dump used is from the operational NAE analysis. The NAE has 0.11° horizontal grid spacing (approximately 12 km) with 70 stretched vertical model levels up to 80 km. The model levels in the MetUM use a terrain-following hybrid-height coordinate that gradually flattens at higher altitudes (Davies *et al.*, 2005). We use the standard time step for this domain of 5 min.

A semi-Lagrangian method does not explicitly conserve any variables. However, the MetUM incorporates an Eulerian discretisation of the continuity equation to ensure local mass conservation (Davies *et al.*, 2005). No explicit diffusion is applied to prognostic variables; the diffusion in the MetUM is entirely implicit and a result of the cubic interpolation (quintic for moisture variables) used in the semi-Lagrangian scheme. The MetUM contains a modified vertical interpolation for θ, described in section 6 of Davies *et al.* (2005), which is required for stability. This modified vertical interpolation is applied up to a height of 3.4 km for our simulation.

The MetUM solves the governing equations of the atmosphere using a 'predictor-corrector' method; an initial 'predictor' is made of the prognostic variables at time level $n+1$ and is refined using a set of 'correctors'. The full method and governing equations are set out by Davies *et al.* (2005) and the inclusion of parametrized physical processes to the equations is presented in Diamantakis *et al.* (2007). We present a simplified description of the method, based on section 5 of Davies *et al.* (2005) and section 2 of Diamantakis *et al.* (2007), so that the budget of PV in the MetUM can be described precisely in the following section.

The discretisation of the governing equations which the MetUM aims to approximate is given by

$$\frac{\mathbf{X}^{n+1} - \mathbf{X}^{n}_{\mathrm{d}}}{\Delta t} = (1-\alpha)(\mathbf{L}+\mathbf{N})^{n}_{\mathrm{d}} + \mathbf{SP}^{n}_{\mathrm{d}} + \alpha(\mathbf{L}+\mathbf{N})^{n+1} + \mathbf{FP}^{n+1}, \quad (1)$$

where $\mathbf{X}$ is a vector of the prognostic variables in the MetUM, $\mathbf{L}$ and $\mathbf{N}$ are the linear and nonlinear dynamics terms respectively, $\mathbf{SP}$ and $\mathbf{FP}$ are the tendencies of the 'slow' and 'fast' parametrized physical processes, a subscript 'd' denotes evaluation at departure points in the MetUM's semi-Lagrangian method, α is a time-weighting coefficient (typically 0.7), n and $n+1$ are the time levels, and Δt is the time step. Figure 1 shows a schematic of a single time step of the MetUM which demonstrates the application of the predictor-corrector method to solving Eq. (1). The components of this figure are now described.

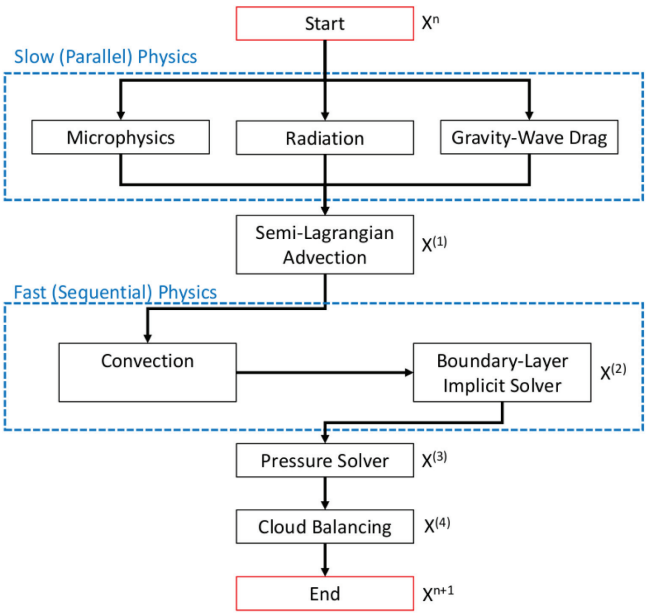

Figure 1. A schematic of a single time step of the MetUM.

First, a set of increments due to the slow physical processes (microphysics, mic, radiation, rad, and gravity-wave drag, gwd) are calculated from the set of prognostic variables at the start of the time step. The increment to prognostic variables due to slow physical processes can be written as

$$\mathbf{SP} \equiv \mathbf{SP}(\mathbf{X}^n). \tag{2}$$

Next, solutions to the thermodynamic, moisture and momentum equations are approximated. This is the predictor step for $\mathbf{X}$. Equation (1) is solved explicitly with time level $n+1$ values replaced with time level n estimates. This can be written as

$$\mathbf{X}^{(1)} = \mathbf{X}^n_{\rm d} + \Delta t\{(1-\alpha)(\mathbf{L}+\mathbf{N})^n_{\rm d} + \alpha(\mathbf{L}+\mathbf{N})^n + \mathbf{SP}^n_{\rm d}\}, \tag{3}$$

where $\mathbf{X}^{(1)}$ is the first estimate of $\mathbf{X}^{n+1}$. Note that the increments due to slow physical processes, interpolated to departure points, are added on at this stage. This predictor step could be split into two stages with an intermediate state of

$$\mathbf{X}^{(1)} = \mathbf{X}^{\rm sl} + \Delta t\, \mathbf{SP}^n_{\rm d}, \tag{4}$$

where $\mathbf{X}^{\rm sl}$ is the set of prognostic variables after the semi-Lagrangian dynamics only and the slow physical processes increments act as the first corrector for $\mathbf{X}$.

The next corrector adds the effects of fast physical processes (convection, con, and boundary layer, bl) using the most up-to-date estimates of the prognostic variables. The fast physical processes are calculated sequentially for stability. This can be written as

$$\mathbf{X}^{(2)} = \mathbf{X}^{(1)} + \Delta t\, \mathbf{FP}(\mathbf{X}^n, \mathbf{X}^{(1)}, \mathbf{X}^{(2)}). \tag{5}$$

At this stage density and Exner pressure have not been updated from their time-level n estimates. The continuity equation is discretised in an Eulerian form and Exner pressure is used to couple the prognostic variables using the ideal gas equation of state. The back substitution of the equations to replace time-level n estimates with $n+1$ values leads to a Helmholtz-type equation to solve; the full equations are given in Appendix B of Davies *et al.* (2005). This is known as the pressure solver and is written as another corrector:

$$\mathbf{X}^{(3)} - \alpha\Delta t\mathbf{L}(\mathbf{X}^{(3)}) = \mathbf{X}^{(2)} + \alpha\Delta t(\mathbf{N}^* - \mathbf{N}^n - \mathbf{L}^n), \tag{6}$$

where $\mathbf{N}^*$ is the latest estimate of $\mathbf{N}$.

At the end of the time step, the MetUM modifies the prognostic variables in clouds to eliminate supersaturation and to account for the additional latent heat release (known as cloud balancing). This can be considered as a final physical process corrector:

$$\mathbf{X}^{(4)} = \mathbf{X}^{(3)} + \Delta t\, \mathbf{CB}(\mathbf{X}^{(3)}), \tag{7}$$

such that $\mathbf{X}^{n+1} \equiv \mathbf{X}^{(4)}$.

2.2. *PV tracers*

A set of PV tracers are integrated online in the MetUM. The method is similar to that developed by Davis *et al.* (1993) and was first applied to the MetUM by Gray (2006). The method works by partitioning and integrating PV. The evolution of PV in Lagrangian form is given by

$$\frac{{\rm D}q}{{\rm D}t} = \frac{1}{\rho}\left\{(\nabla\times\mathbf{u} + 2\boldsymbol{\Omega})\cdot\nabla\dot{\theta} + \nabla\theta\cdot\nabla\times\mathbf{F}\right\}, \tag{8}$$

(Ertel, 1942), where $q = (1/\rho)(\nabla\times\mathbf{u} + 2\boldsymbol{\Omega})\cdot\nabla\theta$ is PV, $\dot{\theta}$ and $\mathbf{F}$ are the diabatic heating and friction respectively, and $\boldsymbol{\Omega}$ is Earth's rotation rate vector.

The general method is to integrate Eq. (8) along trajectories over a forecast of time T:

$$\int_{t=0}^{t=T}\frac{{\rm D}q}{{\rm D}t}{\rm d}t = q(0) + \int_{t=0}^{t=T} S{\rm d}t, \tag{9}$$

where S is the right-hand side of Eq. (8) and is partitioned into different physical processes ($S = \sum S_i$) resulting in a set of PV tracers (q_i) from the integration of S_i starting with each $q_i = 0$.

$$\int_{t=0}^{t=T}\frac{{\rm D}q}{{\rm D}t}{\rm d}t = q(0) + \sum q_i. \tag{10}$$

The PV diagnostics are essentially mimicking the behaviour of the numerical weather prediction model in terms of PV, allowing the tendencies of each parametrized physical process to be partitioned and accumulated separately. There is an implicit assumption here that the effects of each parametrized physical process can be separated. In practice, the PV tracers will often have large cancelling terms between compensating processes. It is important to consider all terms in the PV budget to assess where this is the case.

We partition PV into an advection-only PV tracer ($q_{\rm adv}$) and a set of physics PV tracers ($\sum q_{\rm phys}$). Each PV tracer, apart from the advection-only PV tracer, is set to zero everywhere at the initial time and the advection-only PV tracer is initialised as equal to the PV diagnosed from the prognostic variables $\mathbf{X}$ (diagnosed PV). At the lateral boundaries of a limited-area domain, each PV tracer, apart from the advection-only PV tracer, is set to zero and the advection-only PV is set equal to the diagnosed PV, at each time step. This is because there is no prior information on the history of the air parcels at the lateral boundaries so they are treated like initial conditions.

In the MetUM tracers are advected by the flow resolved in the model using its semi-Lagrangian advection scheme. Passive tracers can also be transported by the effects of sub-grid parametrizations for turbulence and convection. The turbulence scheme acts primarily within the planetary boundary layer and acts as a down-gradient mixing where the diffusion coefficient is dependent upon the Richardson number (Lock *et al.*, 2000). In the simulations shown here, the turbulent diffusion acts in the vertical only. The convection scheme is based on a mass-flux formulation (Gregory and Rowntree, 1990) and passive tracer transport depends upon the diagnosed profile of convective updraught and downdraught mass fluxes. The parametrized subgrid-scale motions have no horizontal component across the sides of a grid

box and, by construction, the updraughts and downdraughts are exactly compensated by vertical motion in the remainder of the column (above the grid box on the Earth's surface) such that the area-averaged vertical motion at each level equals the resolved vertical motion in that grid box.

Although PV is materially conserved in adiabatic, frictionless flows, Haynes and McIntyre (1987) showed that it behaves very differently to a passive tracer once non-conservative processes act. They showed that there can be no net transport of PV across any isentropic surface, even when diabatic and frictional processes are acting. They called this remarkable property the 'PV impermeability theorem' (Haynes and McIntyre, 1990) and it can be regarded as a consequence of Kelvin's circulation theorem. It applies generally to fully compressible non-hydrostatic dynamics and implies that the cross-isentropic flux of PV must be identically zero. This applies to the resolved motions in a model and notional sub-grid transports. Furthermore, the theorem also holds for other vertical coordinates. For example, in pressure coordinates there can be no net transport of the vertical component of vorticity across pressure levels. Therefore, since the sub-grid turbulence and convective schemes describe only vertical fluxes and the non-transport of vorticity must hold, these transport schemes are not applied to the PV tracers and only advection by the resolved 3D motion transports them. The tracer advection scheme in the MetUM also has the option to apply a conservation correction and a monotone correction. However, neither is applied to the PV tracers. The tracer advection scheme simply amounts to updating a variable with its departure-point value, obtained by interpolating the tracer at time-level n to the departure point of the trajectory calculated by the semi-Lagrangian scheme of the MetUM. In this way we are calculating the left-hand side of Eq. (8), partitioned by each PV tracer, at each time step, following the resolved flow of the forecast.

Although there are no PV fluxes across isentropic surfaces, diabatic and frictional effects have an important influence on the PV distribution via diabatic mass fluxes across isentropic surfaces, horizontal divergent flow and frictional torques. Each PV tracer, apart from the advection-only PV tracer, accumulates increments in PV due a specific parametrized physical process at each time step. The PV increment is calculated as the difference in PV before and after adding the increments to the prognostic variables. In this way we are calculating the right-hand side of Eq. (8), partitioned by each parametrized physical process, at each time step.

The slow physical processes are calculated in parallel and each increment is calculated independently using $\mathbf{X}^n$. The increments in PV due to slow physical processes are calculated as

$$\Delta q_{\mathrm{sp}} = q(\mathbf{X}^n + \Delta \mathbf{X}_{\mathrm{sp}}) - q(\mathbf{X}^n), \tag{11}$$

where $q(\cdot)$ means a calculation of PV as a function of the given variables in the argument and sp is microphysics, radiation or gravity-wave drag. The fast physical processes are calculated sequentially so the PV increments are calculated as

$$\Delta q_{\mathrm{con}} = q(\mathbf{X}^{(1)} + \Delta \mathbf{X}_{\mathrm{con}}) - q(\mathbf{X}^{(1)}), \tag{12}$$

for convection and

$$\Delta q_{\mathrm{bl}} = q(\mathbf{X}^{(1)} + \Delta \mathbf{X}_{\mathrm{con}} + \Delta \mathbf{X}_{\mathrm{bl}}) - q(\mathbf{X}^{(1)} + \Delta \mathbf{X}_{\mathrm{con}}), \tag{13}$$

for the boundary-layer scheme, where $q(\mathbf{X}^{(2)}) \equiv q(\mathbf{X}^{(1)} + \Delta \mathbf{X}_{\mathrm{con}} + \Delta \mathbf{X}_{\mathrm{bl}})$. The increment from cloud balancing is also included with the physics PV tracers, calculated as

$$\Delta q_{\mathrm{cloud}} = q(\mathbf{X}^{(4)}) - q(\mathbf{X}^{(3)}). \tag{14}$$

Therefore the equations for updating the PV tracers are given by

$$q^{n+1}_{\mathrm{adv}} = q^{n}_{\mathrm{adv,d}}, \tag{15}$$

for the advection-only PV, where the 'd' subscript indicates that the tracer is evaluated at departure points in the MetUM's semi-Lagrangian scheme:

$$q^{n+1}_{\mathrm{sp}} = (q^{n}_{\mathrm{sp}} + \Delta q_{\mathrm{sp}})_{\mathrm{d}} \tag{16}$$

for slow physical processes, and

$$q^{n+1}_{\mathrm{fp}} = q^{n}_{\mathrm{fp,d}} + \Delta q_{\mathrm{fp}} \tag{17}$$

for fast physical processes, where 'fp' is convection, boundary layer or cloud balancing.

In the previous equations where $q(\cdot)$ is evaluated, we use a modified version of the MetUM's standard diagnostic PV calculation. PV is calculated at the corners of grid points, on model levels where ρ is stored, such that the calculation of the vertical component of vorticity requires no averaging. Each component of PV is calculated using centred differences with prognostic variables averaged when required. The result is then linearly interpolated to the centres of the grid points in the horizontal then linearly interpolated to model levels where θ is stored in the vertical. The modification is that we have also included vertical velocity components in the calculation of PV which improved the PV budget presented later in this article.

2.3. *Case-study*

A 36 h simulation was performed using PV tracers with the MetUM version 7.3 initialised from Met Office operational analysis at 1200 UTC on 28 November 2011. This period corresponds to a case-study from the DIAMET (DIAbatic influences on Mesoscale structures in ExTratropical storms) project (Vaughan *et al.*, 2015) of a double cold front passing over the UK. Diabatic heating and cooling rates in the cold front due to phase changes of water were investigated by Dearden *et al.* (2014) using *in situ* flight data for this case-study. More in-depth details of the meteorological conditions during the case-study are given in Dearden *et al.* (2014).

Our case-study was also included in Chagnon and Gray (2015) (case II) as another example of the tropopause dipole of Chagnon *et al.* (2013) and corresponds to the case with the weakest tropopause dipole, specifically with less diabatically generated positive PV in the stratosphere. We have investigated this case-study to explain the lack of diabatically generated positive PV in the stratosphere using the PV tracer technique. We investigate the effects of the non-conservation of PV by the dynamical core on the tropopause dipole.

2.4. *Trajectories*

PV tracers tell us about the behaviour of physical processes following the resolved flow of the forecast. However, tracer advection schemes on a grid inevitably involve dissipation as features cascade to scales too small to represent. Trajectories calculated from model winds also tell us about processes following the resolved flow of the forecast but do not include any dissipation. We use the trajectory calculation method of Wernli and Davies (1997) (LAGRANTO; Sprenger and Wernli, 2015) with hourly wind data output from the model to provide an alternative view of the forecast flow.

Trajectories are used to calculate PV redistributed by advection as an alternative to the advection-only PV tracer. The advection-only PV tracer at any time tells us the PV that the resolved air parcel had at the start of the model run. PV calculated from trajectories also tells us the PV that the resolved air parcel had at the start of the model run, but is not affected by the numerical diffusion of the tracer advection scheme at each time step. However, it is dependent on the consistency of the trajectory calculations with the MetUM. The trajectory calculations will differ from the model

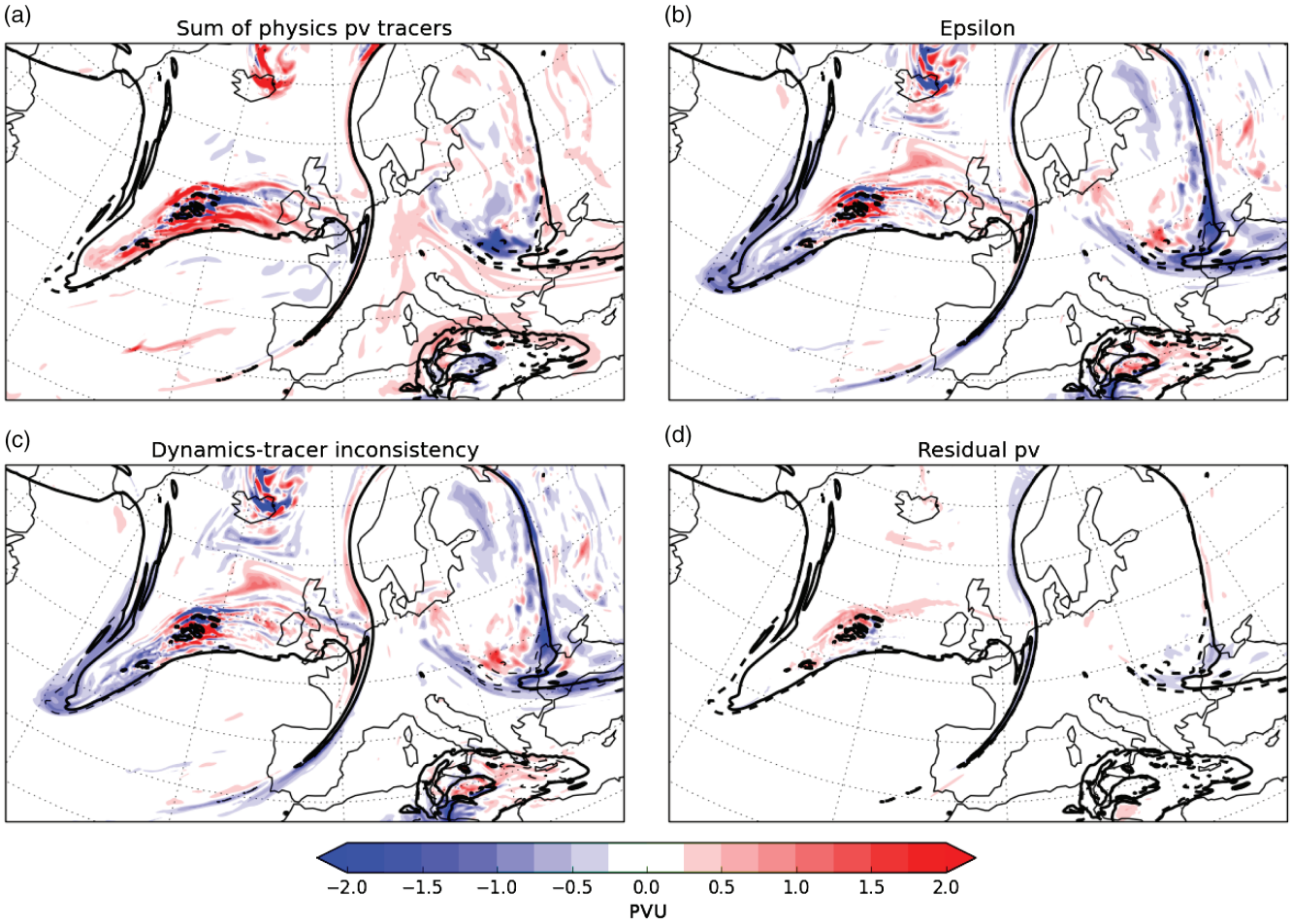

Figure 2. (a) The sum of the physics PV tracers ($\sum q_{\text{phys}}$), (b) ε as defined by Eq. (18), (c) dynamics-tracer inconsistency, and (d) the residual in the PV budget (ε_r in Eq. (33)). All plots are linearly interpolated to the 320 K isentrope for a 36 h forecast. The thick black line in each plot is the 2 PVU contour of the diagnosed PV and the dashed line is the 2 PVU contour of the advection-only PV tracer.

trajectories because of the different numerical schemes used and the lower frequency of data used for the offline calculation of trajectories (hourly).

3. Results

If all processes modifying PV were accounted for by the PV tracers, then the accumulated effects of parametrized physical processes ($\sum q_{\text{phys}}$) would be equivalent to the total change in PV given by the diagnosed PV minus the advection-only PV ($q - q_{\text{adv}}$). We define ε as the difference between these two measures of PV change, such that

$$\varepsilon^n = q^n - q^n_{\text{adv}} - \sum q^n_{\text{phys}}, \tag{18}$$

where $q^n \equiv q(\mathbf{X}^n)$ is the diagnosed PV. Note that ε is the same as q_r in Stoelinga (1996).

Figure 2(b) shows ε and Figure 2(a) shows the sum of physics PV tracers for comparison, each at the end of the 36 h forecast interpolated to the 320 K isentropic surface. The field of ε has structure and amplitude that is comparable to the sum of physics PV tracers and therefore represents an important contribution to the PV budget.

3.1. PV Budget

In this section, by considering the evolution of the PV budget across a time step, we show that ε is completely accounted for by three terms: 'dynamics-tracer inconsistency' ($\Delta\varepsilon_{\text{I}}$) to be defined below based on the inconsistency investigated by Whitehead *et al.* (2015); 'missing PV' ($\Delta\varepsilon_{\text{M}}$) which accounts for any increments in PV not attributed to a dynamical or physical process; and a 'splitting error' ($\Delta\varepsilon_{\text{S}}$) which accounts for the difference between numerical diffusion acting on multiple tracers of PV and the numerical diffusion acting on a single field representing the sum of those PV tracers. In this section we define these three terms mathematically and their numerical form in the MetUM. In principle a PV budget for any numerical model of the atmosphere could be closed using just these three terms.

To calculate a closed PV budget we must account for all changes in PV across a single time step, such that the PV at time level $n+1$ is equal to the PV at time level n plus all the changes in PV in that time step. Considering every change in PV across a single time step of the MetUM (as in Figure 1) we can write:

$$\begin{aligned} q^{n+1} = q^n &+ \{q(\mathbf{X}^{\text{sl}}) - q(\mathbf{X}^n)\} + \{q(\mathbf{X}^{(1)}) - q(\mathbf{X}^{\text{sl}})\} \\ &+ \{q(\mathbf{X}^{(2)}) - q(\mathbf{X}^{(1)})\} + \{q(\mathbf{X}^{(3)}) - q(\mathbf{X}^{(2)})\} \\ &+ \{q(\mathbf{X}^{(4)}) - q(\mathbf{X}^{(3)})\}. \end{aligned} \tag{19}$$

We can attribute each of the terms in Eq. (19) to increments in PV related to dynamical and physical processes. The first increment in PV in Eq. (19) $\{q(\mathbf{X}^{\text{sl}}) - q(\mathbf{X}^n)\}$ is a result of the semi-Lagrangian dynamics, which we can define as Δq_{sl}, such that

$$q(\mathbf{X}^{\text{sl}}) - q(\mathbf{X}^n) = \Delta q_{\text{sl}}. \tag{20}$$

The next increment in PV in Eq. (19) $\{q(\mathbf{X}^{(1)}) - q(\mathbf{X}^{\text{sl}})\}$ is a result of adding the increments to prognostic variables from the slow physical processes to the latest estimate of $\mathbf{X}$. This is approximately equivalent to updating the slow physics PV tracers:

$$q(\mathbf{X}^{(1)}) - q(\mathbf{X}^{\text{sl}}) \approx \sum (q^n_{\text{sp}} + \Delta q_{\text{sp}})_{\text{d}} - \sum q^n_{\text{sp,d}}, \tag{21}$$

where $\sum q_{\rm sp}$ is the set of PV tracers for slow physical processes. The equation is not exact because of the nonlinearity associated with the calculation of the PV increments due to slow physical processes (Eq. (11)) in parallel and the order in which the increments are added. The next increment in PV in Eq. (19),

$$q(\mathbf{X}^{(2)}) - q(\mathbf{X}^{(1)}) = \Delta q_{\rm con} + \Delta q_{\rm bl}, \tag{22}$$

is the increment in PV due to the fast physical processes (Eqs (12) and (13)). The next increment in PV in Eq. (19) $\{q(\mathbf{X}^{(3)}) - q(\mathbf{X}^{(2)})\}$ is a result of the pressure solver, which we can define as $\Delta q_{\rm solver}$, such that

$$q(\mathbf{X}^{(3)}) - q(\mathbf{X}^{(2)}) = \Delta q_{\rm solver}. \tag{23}$$

The final increment in PV in Eq. (19),

$$q(\mathbf{X}^{(4)}) - q(\mathbf{X}^{(3)}) = \Delta q_{\rm cloud}, \tag{24}$$

is the increment in PV due to cloud balancing (Eq. (14)). We can define the increments due to fast physical processes as

$$\sum \Delta q_{\rm fp} = \Delta q_{\rm con} + \Delta q_{\rm bl} + \Delta q_{\rm cloud}. \tag{25}$$

The increment due to cloud balancing $\Delta q_{\rm cloud}$ has been grouped with fast physical processes for convenience.

Whitehead *et al.* (2015) define the inconsistency between a dynamical core and tracer advection as the difference between the evolution of PV calculated by integrating the governing equations in a dynamical core and the advection of a tracer of PV. We can define this 'dynamics-tracer inconsistency' for a single timestep as $\Delta\varepsilon_{\rm I}$ by comparing PV obtained by solving the adiabatic and frictionless governing equations ($q^n + \Delta q_{\rm sl}$) with PV advected using the tracer advection scheme ($q^n_{\rm d}$), such that

$$\Delta\varepsilon_{\rm I} = (q^n + \Delta q_{\rm sl}) - q^n_{\rm d}. \tag{26}$$

Ideally the increment in PV due to the pressure solver from Eq. (23) would be included because the pressure solver involves the solution of the continuity equation and the back-substitution to complete the solution of the thermodynamic and momentum equations. However, the pressure solver also couples the parametrized physics to the dynamics so it is not completely attributable to adiabatic and frictionless dynamics.

With all increments in PV described in terms of dynamics and physics, we can use Eq. (26) to rewrite Eq. (19) as

$$q^{n+1} = q^n_{\rm d} + \sum (q^n_{\rm sp} + \Delta q_{\rm sp})_{\rm d} - \sum q^n_{\rm sp,d} + \sum \Delta q_{\rm fp} + \Delta\varepsilon_{\rm I} + \Delta\varepsilon_{\rm M}, \tag{27}$$

where $\Delta\varepsilon_{\rm M}$ is the 'missing PV' and includes the increment in PV due to the pressure solver as well as accounting for the nonlinearity in the calculations of PV increments due to slow physical processes from Eq. (21).

Rearranging Eq. (18) for time level $n+1$ gives

$$q^{n+1} = q^{n+1}_{\rm adv} + \sum q^{n+1}_{\rm sp} + \sum q^{n+1}_{\rm fp} + \varepsilon^{n+1}, \tag{28}$$

and

$$q^n_{\rm d} = \left(q^n_{\rm adv} + \sum q^n_{\rm sp} + \sum q^n_{\rm fp} + \varepsilon^n\right)_{\rm d}. \tag{29}$$

We can eliminate the terms describing PV tracers in Eq. (27) using the definitions of PV tracer updates (Eqs (15)–(17)). However we first need to account for the difference between numerical diffusion acting on multiple tracers of PV and the numerical diffusion acting on a single field representing the sum of those PV tracers highlighted by the placement of the d subscript in Eq. (29). This 'splitting error' is a result of diffusion in the tracer advection scheme which is entirely implicit for the operational MetUM and in the simulation performed here. We define the 'splitting error' as

$$\Delta\varepsilon_{\rm S} = q^n_{\rm d} - \left(q^n_{\rm adv,d} + \sum q^n_{\rm sp,d} + \sum q^n_{\rm fp,d} + \varepsilon^n_{\rm d}\right). \tag{30}$$

We can now eliminate all terms describing PV tracers in Eq. (27) using Eqs (28)–(30) and the definitions given by Eqs (15)–(17), which gives the result

$$\varepsilon^{n+1} = \varepsilon^n_{\rm d} + \Delta\varepsilon_{\rm I} + \Delta\varepsilon_{\rm M} + \Delta\varepsilon_{\rm S}. \tag{31}$$

Since ε is by definition zero everywhere at the start of a forecast, Eq. (31) tells us that the gap in the PV budget can only be due to the accumulation of the three terms defined in this section: 'dynamics-tracer inconsistency' ($\Delta\varepsilon_{\rm I}$), 'missing PV' ($\Delta\varepsilon_{\rm M}$) and a 'splitting error' ($\Delta\varepsilon_{\rm S}$) and modifications due to the implicit diffusion of ε from carrying it forward on departure points in Eq. (31).

3.2. *Dynamics-tracer inconsistency*

The previous derivation allows us to describe ε completely as the accumulation of three terms: dynamics-tracer inconsistency, missing changes in PV across a single time step, and the difference between advecting a single tracer of PV and advecting multiple tracers of PV. In this section we will show that dynamics-tracer inconsistency is the dominant contribution to ε.

The dynamics-tracer inconsistency is calculated in the MetUM at each time step using Eq. (26). It is then accumulated in the same way as a PV tracer:

$$\varepsilon^{n+1}_{\rm I} = \varepsilon^n_{\rm I,d} + \Delta\varepsilon_{\rm I}. \tag{32}$$

The residual of the PV budget is calculated as

$$\varepsilon^n_{\rm r} = \varepsilon^n - \varepsilon^n_{\rm I}, \tag{33}$$

and can only be due to the 'missing PV' and the 'splitting error' (i.e. the time integral of $\Delta\varepsilon_{\rm M} + \Delta\varepsilon_{\rm S}$). Figure 2 shows the integrated dynamics-tracer inconsistency ($\varepsilon_{\rm I}$) and the residual PV ($\varepsilon_{\rm r}$) for a 36 h forecast. Dynamics-tracer inconsistency accounts for most of ε and the residual PV is generally more than an order of magnitude smaller than ε and has smaller-scale structure. Therefore the pressure solver and nonlinearities in calculations of PV increments ($\Delta\varepsilon_{\rm M}$) and the 'splitting error' ($\Delta\varepsilon_{\rm S}$) are comparatively small contributions to the PV budget for our case-study.

3.3. *Non-conservation of PV by the dynamical core*

In this section we show that the dominant process contributing to dynamics-tracer inconsistency is the non-conservation of PV by the dynamical core rather than the numerical dissipation of a PV tracer in the tracer advection scheme. We have already shown that $\Delta\varepsilon_{\rm S}$ is a small contribution to the PV budget which tells us that the numerical diffusion acting on multiple tracers of PV is approximately the same as the numerical diffusion acting on a single field representing the sum of those PV tracers. In this section we show that the numerical dissipation of a single tracer of PV is small compared to the dynamics-tracer inconsistency.

What is the true change in PV integrated along the resolved flow of the forecast? Dynamics-tracer inconsistency arises both from non-conservation of PV by the dynamical core and the numerical dissipation in the tracer advection scheme. If the tracer advection scheme were perfectly conservative, the total change in PV following an air-mass would be the difference between the diagnosed PV and the PV from the origin of the trajectory that

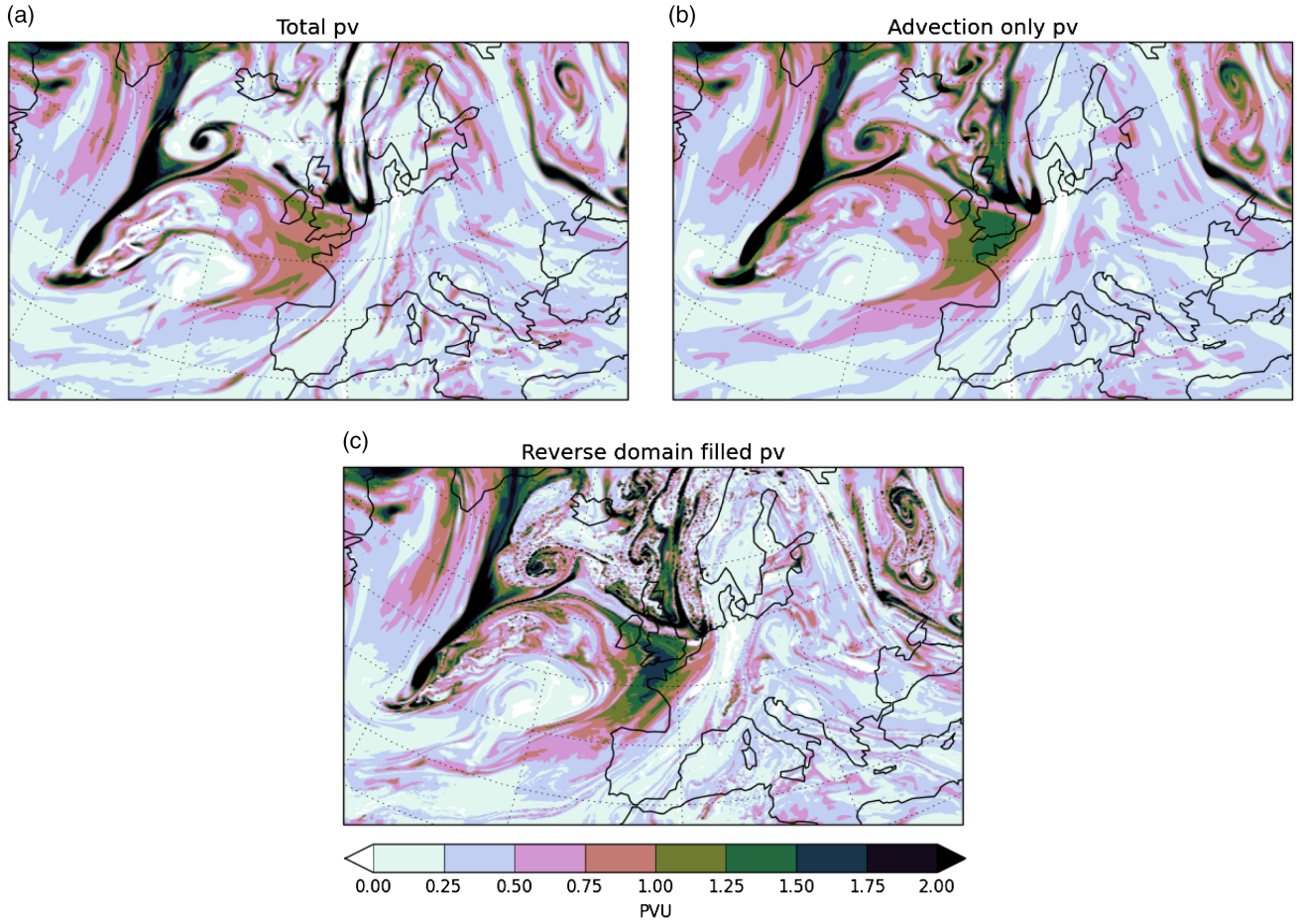

Figure 3. Different measures of PV at 500 hPa at $T + 35$ h: (a) diagnosed PV, (b) advection-only PV tracer, and (c) PV from reverse domain-filling trajectories.

the air-mass followed through the whole forecast ($q - q_{\text{origin}}$). Including the PV at the origin of trajectories in the PV budget (Eq. (18)) gives

$$\varepsilon^n = \left(q^n - q_{\text{origin}} - \sum q^n_{\text{phys}}\right) + (q_{\text{origin}} - q^n_{\text{adv}}), \qquad (34)$$

which highlights a notional partition between non-conservation of PV by the dynamical core (the left bracket) and non-conservation associated with numerical dissipation in the tracer advection scheme acting on the advection-only PV tracer (the right bracket). To estimate the relative magnitudes of these two contributions, trajectories were released from a regular grid on the 500 hPa surface at the end of the forecast ($T + 36$) and calculated backwards in time to the start of the forecast using hourly 3D wind output from the MetUM (section 2.4). The initial PV field is interpolated to each trajectory location at $t = 0$, providing an estimate of q_{origin} which can be associated with the grid point that the trajectory 'arrives on' at the end of the forecast. This technique is called a 'reverse domain filling' (RDF) trajectory calculation since a map of $q_{\text{origin}}(\mathbf{x})$ is obtained (Figure 3(c)).

Figure 3 compares three different measures of PV: the diagnosed PV (q), the advection-only PV (q_{adv}), and the PV calculated from RDF trajectories (q_{origin}). The fields are shown at 500 hPa because the back-trajectory calculations were initialised on pressure levels. The 500 hPa surface is found using linear interpolation while assuming a logarithmic variation of pressure with height consistent with other MetUM diagnostics. Owing to the exact conservation implied by the RDF technique, the maxima and minima in the field are given by the extrema in the initial PV distribution (at the origin locations which in general are not at 500 hPa due to vertical motion). Fine scales are generated through stirring by advection and there is no dissipation in the reverse domain-filling calculation to smooth the small-scale structure. In contrast, the advection-only tracer experiences numerical diffusion. This acts to remove the smallest structures and to fill in some regions with intermediate PV values (for example, around the cyclonic spiral to the southwest of Iceland in Figure 3). The highest PV values in RDF PV over southern England are also reduced in the PV tracer, presumably by mixing in the tracer calculation. In contrast, the diagnosed PV (from the prognostic variables) shows much lower values than q_{adv} or q_{origin} within the low-PV air to the south of Iceland. Part of this difference is associated with physical processes and part with the non-conservation by the dynamical core.

Figure 4 shows ε calculated from Eq. (18) and ε calculated from the first bracket in Eq. (34) using the RDF estimate q_{origin}. There are considerable differences between the two terms, mainly due to fine-scale structure fluctuating about zero. As already discussed, the fine-scale structure arises from lack of dissipation in the RDF calculation and also small errors associated with the offline calculation of long trajectories used in the RDF calculation. However, it can be seen that ε calculated from RDF trajectories accounts for most of the larger-scale and -magnitude PV anomalies seen in ε calculated from Eq. (18). Therefore, we can conclude that numerical diffusion of the advection-only PV tracer is not the major contribution to the dynamics-tracer inconsistency in ε.

Tracer advection within the MetUM has the option to run with various different interpolation schemes. Running the same simulation while varying the interpolation scheme used for the PV tracers from linear to quintic makes very little difference to the dynamics-tracer inconsistency (not shown). This suggests that the numerical diffusion of the PV tracers associated with the interpolation to departure points in the semi-Lagrangian advection scheme is not the major contribution to the dynamics-tracer inconsistency.

Having eliminated other options, the conclusion is that the tracer advection used for the PV tracers is more conservative,

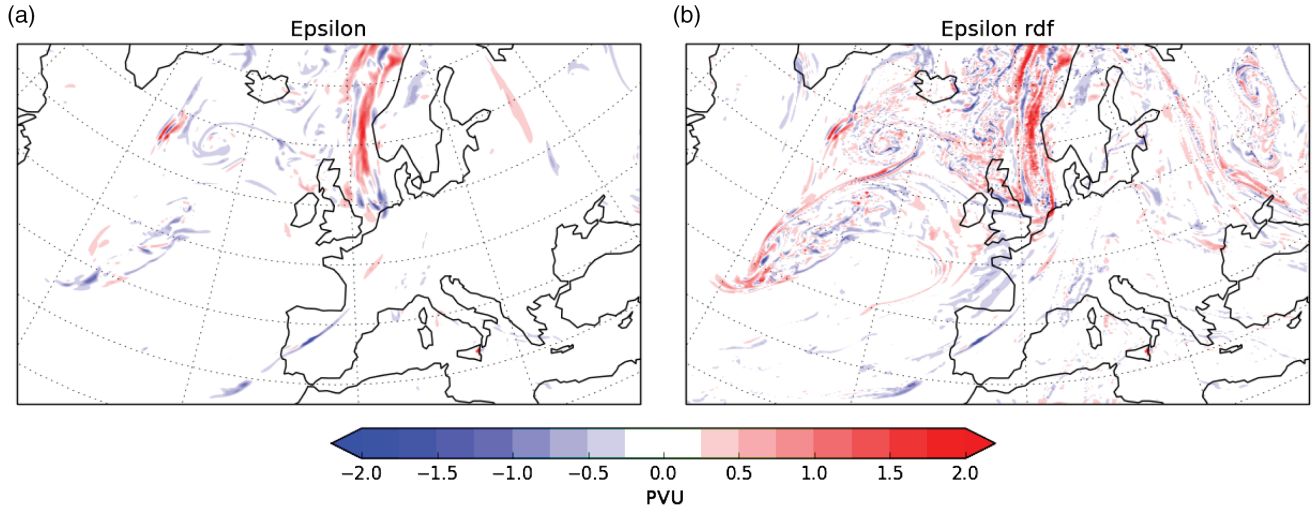

Figure 4. The difference between the accumulated effects of parametrized physical processes ($\sum q_{\text{phys}}$) and the total change in PV calculated using (a) advection-only PV (q_{adv}) and (b) PV traced back along a trajectory (q_{origin}), at 500 hPa and T + 35 h.

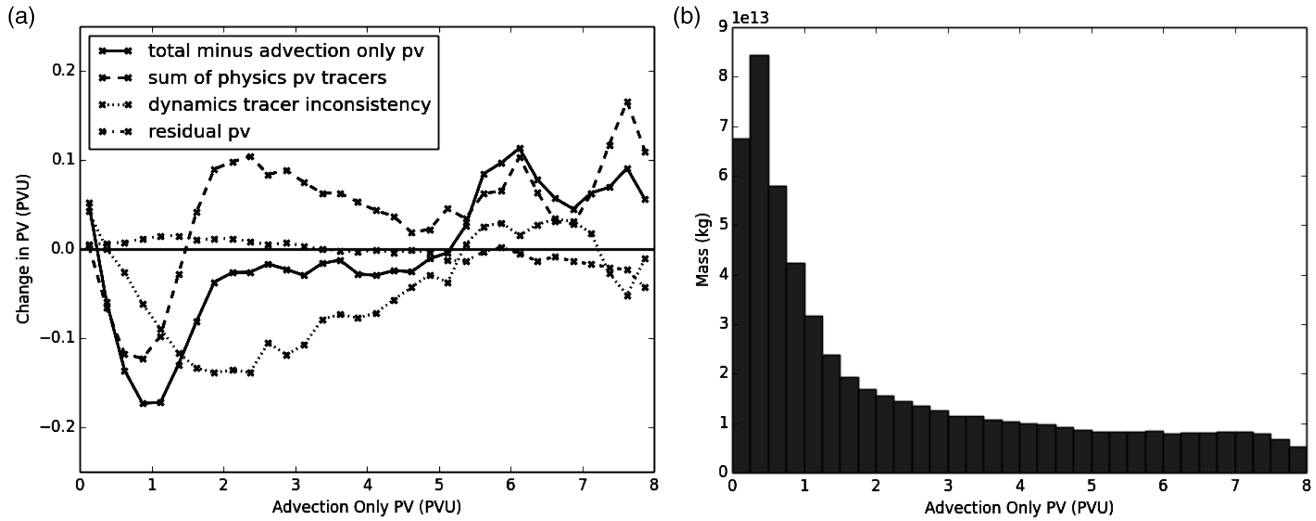

Figure 5. (a) The near-tropopause mass-weighted average PV in bins of 0.25 PVU of the advection-only PV tracer. (b) The total mass in each 0.25 PVU bin of advection-only PV. Results are shown for an integration time of 36 h.

in terms of PV, than the dynamical core. The majority of the dynamics-tracer inconsistency must therefore be due to the non-conservation of PV by the dynamical core.

How should we interpret this non-conservation of PV by the dynamical core? Like PV, θ is conserved in the absence of diabatic and frictional processes. Therefore it can be partitioned into a set of tracers in the same way as PV (Martínez-Alvarado and Plant, 2014) and will also have an associated dynamics-tracer inconsistency. However, θ is a prognostic variable in the MetUM so the changes to θ in the dynamical core are essentially identical to tracer advection (depending on the interpolation schemes used). The dynamics-tracer inconsistency for θ (calculated with Eq. (26)) would therefore be close to zero and tests have shown it is indeed close to zero (O. Martínez-Alvarado, 2015; personal communication).

If we were to run the same study as Whitehead *et al.* (2015) with the MetUM we would get different answers depending on whether we use PV or θ. The prognostic variable θ tells us that the MetUM has a consistent dynamical core and tracer advection scheme. However, the diagnostic variable PV shows a large dynamics-tracer inconsistency. PV is diagnosed as a function of the gradients of the prognostic variables, each of which are updated separately (Eq. (1)). Therefore the Lagrangian equation for PV (Eq. (8)) is not respected exactly by the dynamical core of the MetUM. The dissipation of prognostic variables θ and $\mathbf{u}$ in the dynamical core will act like the effects of heating and friction terms on PV.

We could also associate the non-conservation of PV by the dynamical core to an implicit representation of physical processes at small scales. Kunkel *et al.* (2014) used a PV tracer in an adiabatic and frictionless simulation to assess the impact of inertia-gravity waves near the tropopause. Kunkel *et al.* (2014) found systematic differences between the diagnosed PV and tracer PV in the regions of inertia-gravity waves. Small-scale physical processes would act to modify PV but should not be expected to modify passive tracers in the same way.

3.4. *Tropopause dipole*

Using the PV tracers method Chagnon *et al.* (2013) showed that the accumulated effects of parametrized physical processes contributed to a sharpening of the tropopause PV gradient for a case-study of an extratropical cyclone. In this section we investigate the effects of the non-conservation of PV by the dynamical core on the tropopause PV gradient for our case-study.

Chagnon *et al.* (2013) showed, for their case-study, that the 2 PVU surface of the advection-only PV tracer coincided with the 2 PVU surface of the diagnosed PV. This meant that the direct modifications of PV by non-conservative processes did not act to change the position of the tropopause. They showed that,

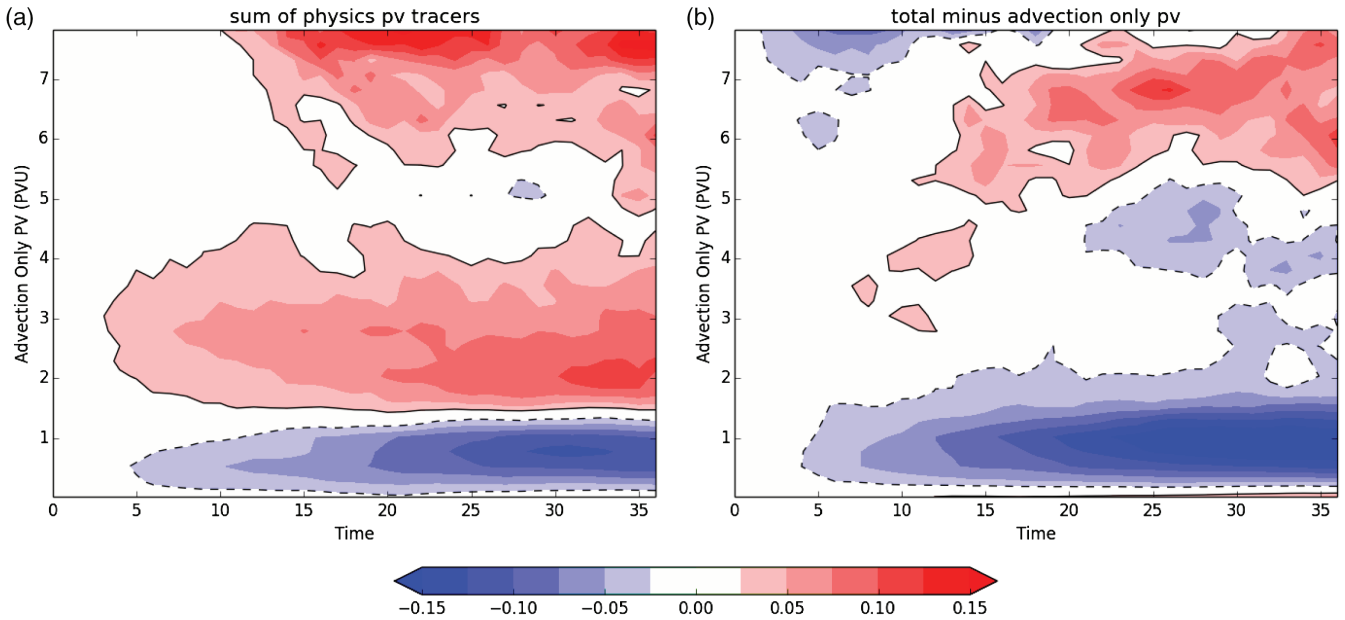

Figure 6. The near-tropopause mass-weighted average PV in bins of 0.25 PVU of the advection-only PV tracer against time (hours since forecast initialisation) for (a) the accumulated effects of parametrized physical processes ($\sum q_{\text{phys}}$) and (b) the total change in PV ($q - q_{\text{adv}}$). The solid and dashed lines show positive and negative anomalies respectively.

by summing the values of the near tropopause total change in PV ($q - q_{\text{adv}}$), binned by the advection-only PV tracer, that the average change in PV for values of advection-only PV less than 2 PVU (tropospheric) was negative and the average change in PV for values of advection-only PV greater than 2 PVU (stratospheric) was positive with a zero value at 2 PVU (Figure 6 in Chagnon *et al.*, 2013). Chagnon and Gray (2015) repeated this diagnostic for three more extratropical cyclones. They showed that our case-study (case II in Chagnon and Gray, 2015) contains regions of tropopause sharpening but the average strength of the tropopause dipole is weaker and the dipole does not have a strong positive stratospheric PV modification.

Figure 5(a) shows the same diagnostic as Figure 6 in Chagnon *et al.* (2013) but integrated over many vertical levels by weighting the gridpoints by mass rather than an area average over individual vertical levels, with Figure 5(b) showing the total mass associated with each bin. The diagnostic was integrated over many vertical levels so that we do not miss any shallow PV anomalies that may be important. We also include only gridpoints within 2.5 km of the tropopause (in the vertical), excluding the boundary layer using the MetUM's diagnosis of boundary-layer height. The mean mass of the included gridpoints is 3.18×10^{10} kg, with a maximum of 4.21×10^{10} kg and a minimum of 5.69×10^{9} kg.

Whitehead *et al.* (2015) found large amounts of dynamics-tracer inconsistency where isentropes intersected the ground. We find the same result for our case-study. However, this low-level 'dynamics-tracer' inconsistency is found to largely cancel out tendencies between the radiation and boundary-layer parametrization schemes such that the total change in PV ($q - q_{\text{adv}}$) is much smaller in magnitude. By excluding the boundary layer, we avoid seeing large signals of opposite sign in Figure 5(a).

Figure 5(a) does show a dipole in the total change in PV. The dipole is consistent with the one in Chagnon and Gray (2015) with the addition of a positive PV anomaly at q_{adv} between 6 and 8 PVU which can be attributed to the use of many vertical levels. More relevant to this study is the large difference between the sum of physics PV tracers and the total change in PV ($q - q_{\text{adv}}$). This difference is mostly accounted for by the non-conservation of PV by the dynamical core (ε_{I}). In Figure 2 there is a difference between the position of the 2 PVU contour of the advection-only PV and the 2 PVU contour of the diagnosed PV that is directly caused by the non-conservation of PV by the dynamical core. The movement of the 2 PVU contour agrees with Figure 5 in which the zero point of the total change in PV is found at values of the advection-only PV tracer that are greater than 2 PVU but the sum of physics PV tracers still crosses zero close to 2 PVU. The difference can be attributed to the systematic reduction of PV by the dynamical core.

Figure 6 shows the same diagnostic as Figure 5 as a function of lead time for the accumulated effects of parametrized physical processes and the total change in PV. The difference between Figure 6(a) and (b) can be attributed to the non-conservation of PV by the dynamical core (ϵ_{I}). The sum of physics PV tracers shows a clear dipole at a value of advection-only PV tracer close to the 2 PVU tropopause; however this is not present for the total change in PV which appears to have a faint dipole which drifts with time. This suggests that the non-conservation of PV by the dynamical core acts to move the 2 PVU tropopause position whereas the parametrized physical processes do not.

4. Conclusions

A new diagnostic framework is introduced to calculate the non-conservation of PV by the dynamical core of a numerical model of the atmosphere when simulating a realistic case-study with a full suite of physics parametrizations. The non-conservation of PV by the dynamical core has been considered in the context of PV tracers based on the method introduced by Davis *et al.* (1993). Whitehead *et al.* (2015) used tracers of PV to diagnose inconsistencies between dynamical cores and tracer advection schemes but applied to idealised simulations without any parametrization of physical processes. A 'dynamics-tracer inconsistency' diagnostic has been incorporated into the PV tracers method in the MetUM and used to diagnose the non-conservation of PV by the dynamical core. We have shown that, for our case-study, the non-conservation of PV by the dynamical core has a comparable contribution to the PV budget to that of parametrized physical processes. Similar results have also been produced with the dynamics-tracer inconsistency diagnostic in other case-studies (not shown).

Discrepancies between the PV diagnosed from the prognostic variables of a model and the PV tracers have been previously noted. Davis *et al.* (1993) attributed the difference to numerical errors in the explicit integration of PV. Stoelinga (1996) attributed the difference to using a numerical model that does not conserve

PV explicitly. Gray (2006) and Chagnon *et al.* (2013) attributed the difference to the amplified effects of diffusion across multiple tracers. In reality, all of these terms could be important and will have differing importance for different numerical models. We have introduced a framework that can account for each of these effects separately and we can calculate the relative importance of these terms for the PV tracers method applied to any numerical weather prediction model.

The residual in the PV budget is generally more than an order of magnitude smaller than the dominant physical processes when the non-conservation of PV by the dynamical core is accounted for. Currently the largest part of the residual in the PV budget comes from the pressure solver. If the residual in the PV budget were larger, then a method to sensibly partition the PV increment from the pressure solver would need to be developed for the PV tracers. A possible method to include the pressure solver would be to run two time steps of the model in parallel: one regular time step and one adiabatic and frictionless time step. The latter would be used to calculate the dynamics PV increments in calculating the dynamics-tracer inconsistency. This method is generic for any dynamical core and would also be a closer match to the inconsistency defined by Whitehead *et al.* (2015). It has not been attempted for this study because the dynamics-tracer inconsistency diagnosed from the semi-Lagrangian dynamics step was the major term missing from the PV budget.

The version of the MetUM (7.3) used in this study does not add any explicit diffusion to the PV tracers. In the initial formulation of the PV tracers method, Davis *et al.* (1993) chose to add diffusion to the PV increments at each time step to mimic the effect of explicit thermal diffusion on small-scale anomalies. Our approach is to use the PV tracers to assess the behaviour of the numerical model itself.

An advantage of the PV tracers is that the cumulative effects of different processes can be quantified in a single simulation, as opposed to model sensitivity studies where the different experiments will in general have different model trajectories. This is important because the processes interact nonlinearly and so each process depends sensitively upon the model trajectory. The technique could be used to relate forecast errors to the processes contributing and to identify systematic model error.

It has been shown that numerical weather prediction models systematically smooth the tropopause PV gradient with lead time (Gray *et al.*, 2014). Gray *et al.* (2014) hypothesised that the smoothing of the PV gradient was due to an under-representation of diabatic processes consistent with the development of a diabatic PV dipole shown by Chagnon *et al.* (2013). However we have shown that the the non-conservation of PV by the dynamical core has a strong effect on the tropopause and could also explain the smoothing of the PV gradient. The results of Chagnon *et al.* (2013) and Chagnon and Gray (2015) do implicitly include the non-conservation of PV by the dynamical core because they look at differences between the diagnosed and advection-only PV. However, by attributing PV to dynamics-tracer inconsistency, we have reduced the uncertainty in the PV budget and therefore reduced the uncertainty in the individual PV tracers, further validating the approach in Chagnon *et al.* (2013) of looking at the effects of individual physical processes on the PV dipole with the caveat that the non-conservation of PV by the dynamical core should also be considered.

By looking at the evolution of numerical solutions to idealised cases of frontogenesis past the point of frontal collapse, Visram *et al.* (2014) suggested that insufficient Lagrangian conservation of PV can cause a degradation to the long-term solutions of forecasts. The non-conservation of PV by the dynamical core would be a direct cause of this. However, we refrain from describing the non-conservation of PV by the dynamical core as 'model error' because it is necessary to have some form of dissipation in numerical models of the atmosphere and this dissipation may also be linked to unrepresented small-scale physical processes. By diagnosing non-conservation of PV by the dynamical core with the dynamics-tracer inconsistency diagnostic, we can assess the Lagrangian conservation of PV in case-studies and differentiate between physical processes and model error.

Acknowledgements

The lead author is funded by a Natural Environment Research Council doctoral training grant (reference NE/L501608/1) and is grateful for CASE funding from the Met Office with Keith Williams as supervisor. We would like to thank Terry Davies for sharing his expert knowledge of the MetUM through various discussions and his help in making sure the equations were correctly presented. We are also thankful to Oscar Martínez-Alvarado and Jeffrey Chagnon for all the technical and conceptual help with the PV tracers. We would like to thank two anonymous reviewers for improving this article with their helpful suggestions. We acknowledge use of the MONSooN system, a collaborative facility supplied under the Joint Weather and Climate Research Programme which is a strategic partnership between the Met Office and the Natural Environment Research Council. The edits required for the PV tracers are stored as a branch edit in PUMA's TRAC system. The branch used in this article is /dev/LSaffin/vn7.3_PV_Tracers revision number 18699.

Appendix

Notation

Table A1 shows the notation used in this article.

Table A1.

Symbol	Description
q	PV
q_{adv}	Advection-only PV
q_{phys}	PV due to a parametrized physical process
q_{sp}	PV due to a parametrized slow physical process
q_{fp}	PV due to a parametrized fast physical process
q_{origin}	PV at the start of an air mass trajectory
ε	Difference between the accumulated effects of parametrized physical processes and the total change in PV
ε_{I}	Contribution to ε due to inconsistency in PV between the dynamical core and tracer advection
ε_{M}	Contribution to ε due to missing terms in PV over a single timestep
ε_{S}	Contribution to ε due to the amplified numerical diffusion by splitting PV into multiple tracers
ε_{r}	Residual PV
$\mathbf{X}$	A vector of the prognostic variables in the MetUM
$\mathbf{X}^{(1)},\mathbf{X}^{(2)},\ldots$	The 1st, 2nd, ... predictor of $\mathbf{X}^{n+1}$

References

Chagnon JM, Gray SL. 2015. A diabatically generated potential vorticity structure near the extratropical tropopause in three simulated extratropical cyclones. *Mon. Weather Rev.* **143**: 2337–2347, doi: 10.1175/MWR-D-14-00092.1.

Chagnon JM, Gray SL, Methven J. 2013. Diabatic processes modifying potential vorticity in a North Atlantic cyclone. *Q. J. R. Meteorol. Soc.* **139**: 1270–1282, doi: 10.1002/qj.2037.

Charney J. 1955. The use of the primitive equations of motion in numerical prediction. *Tellus* **7**: 22–26, doi: 10.1111/j.153-3490.1955.tb01138.x.

Davies T. 2013. Lateral boundary conditions for limited-area models. *Q. J. R. Meteorol. Soc.* **140**: 185–196, doi: 10.1002/qj.2127.

Davies T, Cullen MJP, Malcolm AJ, Mawson MH, Staniforth A, White AA, Wood N. 2005. A new dynamical core for the Met Office's global and regional modelling of the atmosphere. *Q. J. R. Meteorol. Soc.* **131**: 1759–1782, doi: 10.1256/qj.04.101.

Davis CA, Emanuel KA. 1991. Potential vorticity diagnostics of cyclogenesis. *Mon. Weather Rev.* **119**: 1929–1953.

Davis CA, Stoelinga MT, Kuo YH. 1993. The integrated effect of condensation in numerical simulations of extratropical cyclogenesis. *Mon. Weather Rev.* **121**: 2309–2330.

Davis CA, Grell ED, Shapiro MA. 1996. The balanced dynamical nature of a rapidly intensifying oceanic cyclone. *Mon. Weather Rev.* **124**: 3–26.

Dearden C, Connolly PJ, Lloyd G, Crosier J, Bower KN, Choularton TW, Vaughan G. 2014. Diabatic heating and cooling rates derived from in-situ microphysics measurements: A case study of a wintertime UK cold front. *Mon. Weather Rev.* **142**: 3100–3125, doi: 10.1175/MWR-D-14-00048.1.

Diamantakis M, Davies T, Wood N. 2007. An iterative time-stepping scheme for the Met Office's semi-implicit semi-Lagrangian non-hydrostatic model. *Q. J. R. Meteorol. Soc.* **133**: 997–1011, doi: 10.1002/qj.59.

Edwards JM, Slingo A. 1996. Studies with a flexible new radiation code. I: Choosing a configuration for a large-scale model. *Q. J. R. Meteorol. Soc.* **122**: 689–719, doi: 10.1002/qj.49712253107.

Ertel H. 1942. Ein neuer hydrodynamischer Wirbelsatz. *Meteorol. Z.* **59**: 277–281.

Gray SL. 2006. Mechanisms of midlatitude cross-tropopause transport using a potential vorticity budget approach. *J. Geophys. Res.* **111**: D17 113, doi: 10.1029/2005JD006259.

Gray SL, Dunning CM, Methven J, Masato G, Chagnon JM. 2014. Systematic model forecast error in Rossby wave structure. *Geophys. Res. Lett.* **41**: 2979–2987, doi: 10.1002/2014GL059282.

Gregory D, Rowntree PR. 1990. A mass flux convection scheme with representation of cloud ensemble characteristics and stability-dependent closure. *Mon. Weather Rev.* **118**: 1483–1506.

Haynes PH, McIntyre ME. 1987. On the evolution of vorticity and potential vorticity in the presence of diabatic heating and frictional or other forces. *J. Atmos. Sci.* **44**: 828–841.

Haynes PH, McIntyre ME. 1990. On the conservation and impermeability theorems for potential vorticity. *J. Atmos. Sci.* **47**: 2021–2031.

Hoskins BJ, McIntyre ME, Robertson AW. 1985. On the use and significance of isentropic potential vorticity maps. *Q. J. R. Meteorol. Soc.* **111**: 877–946, doi: 10.1002/qj.49711147002.

Kunkel D, Hoor P, Wirth V. 2014. Can inertia-gravity waves persistently alter the tropopause inversion layer? *Geophys. Res. Lett.* **41**: 7822–7829, doi: 10.1002/2014GL061970.

Lock AP, Brown AR, Bush MR, Martin GM, Smith RNB. 2000. A new boundary-layer mixing scheme. Part I: Scheme description and single-column model tests. *Mon. Weather Rev.* **128**: 3187–3199.

McIntyre ME, Norton WA. 2000. Potential vorticity inversion on a hemisphere. *J. Atmos. Sci.* **57**: 1214–1235.

Martnez-Alvarado O, Plant RS. 2014. Parametrized diabatic processes in numerical simulations of an extratropical cyclone. *Q. J. R. Meteorol. Soc.* **140**: 1742–1755, doi: 10.1002/qj.2254.

Reed RJ. 1955. A study of a characteristic type of upper-level frontogenesis. *J. Meteorol.* **12**: 226–237.

Scaife AA, Butchart N, Warner CD, Swinbank R. 2002. Impact of a spectral gravity wave parameterization on the stratosphere in the Met Office unified model. *J. Atmos. Sci.* **59**: 1473–1489.

Sprenger M, Wernli H. 2015. The LAGRANTO Lagrangian analysis tool – version 2.0. *Geosci. Model Dev.* **8**: 2569–2586, doi: 10.5194/gmdd-8-1893-2015.

Stoelinga MT. 1996. A potential vorticity-based study of the role of diabatic heating and friction in a numerically simulated baroclinic cyclone. *Mon. Weather Rev.* **124**: 849–874.

Vaughan G, Methven J, Anderson D, Antonescu B, Baker L, Baker TP, Ballard SP, Bower KN, Brown PRA, Chagnon J, Choularton TW, Chylik J, Connolly PJ, Cook PA, Cotton RJ, Crosier J, Dearden C, Dorsey JR, Frame THA, Gallagher MW, Goodliff M, Gray SL, Harvey BJ, Knippertz P, Lean HW, Li D, Lloyd G, Martínez-Alvarado O, Nicol J, Norris J, Öström E, Owen J, Parker DJ, Plant RS, Renfrew IA, Roberts NM, Rosenberg P, Rudd AC, Schultz DM, Taylor JP, Trzeciak T, Tubbs R, Vance AK, van Leeuwen PJ, Wellpott A, Woolley A. 2015. Cloud banding and winds in intense European cyclones: Results from the DIAMET project. *Bull. Am. Meteorol. Soc.* **96**: 249–265, doi: 10.1175/BAMS-D-13-00238.1.

Visram AR, Cotter CJ, Cullen MJP. 2014. A framework for evaluating model error using asymptotic convergence in the Eady model. *Q. J. R. Meteorol. Soc.* **140**: 1629–1639, doi: 10.1002/qj.2244.

Webster S, Brown AR, Cameron DR, Jones CP. 2003. Improvements to the representation of orography in the Met Office Unified Model. *Q. J. R. Meteorol. Soc.* **129**: 1989–2010, doi: 10.1256/qj.02.133.

Wernli H, Davies HC. 1997. A Lagrangian-based analysis of extratropical cyclones. I: The method and some applications. *Q. J. R. Meteorol. Soc.* **123**: 467–489, doi: 10.1002/qj.49712353811.

Whitehead JP, Jablonowski C, Kent J, Rood RB. 2015. Potential vorticity: measuring consistency between GCM dynamical cores and tracer advection schemes. *Q. J. R. Meteorol. Soc.* **141**: 739–751, doi: 10.1002/qj.2389.

Wilson DR, Ballard SP. 1999. A microphysically based precipitation scheme for the UK Meteorological Office Unified Model. *Q. J. R. Meteorol. Soc.* **125**: 1607–1636, doi: 10.1002/qj.49712555707.

Zhang K, Wan H, Wang B, Zhang M. 2008. Consistency problem with tracer advection in the atmospheric model GAMIL. *Adv. Atmos. Sci.* **25**: 306–318, doi: 10.1007/s00376-008-0306-z.